Lawrence Berkeley National Laboratory

Lawrence Berkeley National Laboratory

Title

The coexistence curve of finite charged nuclear matter

Permalink

https://escholarship.org/uc/item/31x9c12x

Authors

Elliott, J.B.
Moretto, L.G.
Phair, L.
et al.

Publication Date

2001

eScholarship.org Powered by the California Digital Library
University of California

The coexistence curve of finite charged nuclear matter

J. B. Elliott[*], L. G. Moretto[*], L. Phair[*], G. J. Wozniak[*], L. Beaulieu[†], H. Breuer[**], R. G. Korteling[‡], K. Kwiatkowski[§], T. Lefort[¶], L. Pienkowski[‖], A. Ruangma[††], V. E. Viola[¶], S. J. Yennello[††], S. Albergo[‡‡], F. Bieser[§§], F. P. Brady[¶¶], Z. Caccia[‡‡], D. A. Cebra[¶¶], A. D. Chacon[***], J. L. Chance[¶¶], Y. Choi[†††], S. Costa[‡‡], M. L. Gilkes[†††], J. A. Hauger[†††], A. S. Hirsch[†††], E. L. Hjort[†††], A. Insolia[‡‡], M. Justice[‡‡‡], D. Keane[‡‡‡], J. C. Kintner[¶¶], V. Lindenstruth[§§§], M. A. Lisa[§§], H. S. Matis[§§], M. McMahan[§§], C. McParland[§§], W. F. J. Müller[§§§], D. L. Olson[§§], M. D. Partlan[¶¶], N. T. Porile[†††], R. Potenza[‡‡], G. Rai[§§], J. Rasmussen[§§], H. G. Ritter[§§], J. Romanski[‡‡], J. L. Romero[¶¶], G. V. Russo[‡‡], H. Sann[§§§], R. P. Scharenberg[†††], A. Scott[‡‡‡], Y. Shao[‡‡‡], B. K. Srivastava[†††], T. J. M. Symons[§§], M. Tincknell[†††], C. Tuvé[‡‡], S. Wang[‡‡‡], P. Warren[†††], H. H. Wieman[§§], T. Wienold[§§] and K. Wolf[***]

[*]*Nuclear Science Division, Lawrence Berkeley National Laboratory, University of California, Berkeley, CA 94720*
[†]*ISiS Collaboration, Départment de Physique, Université Laval Québec, Canada G1K 7P4*
[**]*ISiS Collaboration, Department of Physics, University of Maryland, College Park, MD 20740*
[‡]*ISiS Collaboration, Department of Chemistry, Simon Fraser University, Burnaby, British Columbia, Canada V5A IS6*
[§]*ISiS Collaboration, Los Alamos National Laboratory, Physics Division p-23, Los Alamos, NM 87545*
[¶]*ISiS Collaboration, Department of Chemistry and IUCF, Indiana University, Bloomington, Indiana 47405*
[‖]*ISiS Collaboration, Heavy Ion Laboratory, Warsaw University, Warsaw, Poland*
[††]*ISiS Collaboration, Department of Chemistry & Cyclotron Laboratory, Texas A&M University, College Station, TX 77843*
[‡‡]*EOS Collaboration, Universitá di Catania and Istituto Nazionale di Fisica Nucleare-Sezione di Catania, 95129 Catania, Italy*
[§§]*EOS Collaboration, Nuclear Science Division, Lawrence Berkeley National Laboratory, Berkeley, CA 94720*
[¶¶]*EOS Collaboration, University of California, Davis, CA 95616*
[***]*EOS Collaboration, Texas A&M University, College Station, TX 77843*
[†††]*EOS Collaboration, Purdue University, West Lafayette, IN 47907*
[‡‡‡]*EOS Collaboration, Kent State University, Kent, OH 44242*
[§§§]*EOS Collaboration, GSI, D-64220 Darmstadt, Germany*

Abstract. The multifragmentation data of the ISiS Collaboration and the EOS Collaboration are examined. Fisher's droplet formalism, modified to account for Coulomb energy, is used to determine the critical exponents τ and σ, the surface energy coefficient c_0, the pressure-temperature-density coexistence curve of finite nuclear matter and the location of the critical point.

This work examines the formation of "fragments" from excited nuclei, termed "nuclear multifragmentation," which may be the result of a liquid-vapor phase transition [1, 2, 3]. Past analyses of nuclear multifragmentation have determined critical exponents [1, 4], examined caloric curves [5] and reported negative heat capacities [6]. This work will show that three EOS experimental data sets and the ISiS data set contain a signature of a liquid-vapor phase transition manifested by the scaling behavior of Fisher's droplet formalism. Via Fisher's scaling the coexistence line

TABLE 1. Fit parameters

System	τ	σ	β	c_0 (MeV)	$\Delta\mu$ (AMeV)	x	y
ISiS $\pi+$ Au	2.18 ± 0.14	0.54 ± 0.01	0.33 ± 0.25	18.3 ± 0.5	0.06 ± 0.03	1.0 ± 0.06	1.00 (fixed)
EOS Au + C	2.2 (fixed)	0.69 ± 0.02	0.30 ± 0.01	14 ± 1	0.38 ± 0.02	1.0 ± 0.1	0.43 ± 0.06
EOS La + C	2.2 (fixed)	0.69 ± 0.02	0.30 ± 0.01	14 ± 1	0.42 ± 0.03	1.2 ± 0.1	0.33 ± 0.08
EOS Kr + C	2.2 (fixed)	0.69 ± 0.02	0.30 ± 0.01	14 ± 1	0.61 ± 0.05	3.9 ± 0.7	0.70 ± 0.20

is observed over a large temperature interval extending up to and including the critical point. Critical exponents τ and σ, the critical temperature T_c, the surface energy coefficient c_0, the compressibility factor C_F, the pressure-density-temperature coexistence curve and a measure of the critical pressure p_c and critical density ρ_c can be determined.

The Indiana Silicon Sphere (ISiS) Collaboration collected over $1,000,000$ events for the reaction 8.0 GeV/c $\pi+$ Au. For every event the fragment charge distribution was recorded for $1 \leq Z \leq 15$, fragments with $Z > 15$ were not elementally resolved [7]. Particles knocked out of the gold nucleus in the projectile-target collision were differentiated from the fragments formed from the excited remnant via a charge dependent kinetic energy cut [8]. An estimate was made of the charge of the fragmenting system Z_0 by subtracting the charge of the knockout particles from the charge of the gold nucleus. The mass of the fragmenting system A_0 was estimated by assuming that 1.7 were neutrons knocked from the gold nucleus for every proton. The excitation energy per nucleon of the remnant E^* was constructed via energy balance considerations and the data was binned in terms of E^* in units of tenth of an AMeV.

The EOS Collaboration collected $\sim 25,000$ fully reconstructed events ($76 \leq Z_{observed} \leq 82$) for the reaction 1.0 AGeV Au + C, $\sim 22,000$ fully reconstructed events ($54 \leq Z_{observed} \leq 60$) for 1.0 AGeV La + C and $\sim 36,000$ fully reconstructed events ($32 \leq Z_{observed} \leq 39$) for 1.0 AGeV Kr + C [9]. For every event, the charge and mass of the projectile remnant (Z_0, A_0) were determined by subtracting the charge and mass of the particles knocked out of the projectile from the charge and mass of the projectile. The knockout particles were distinguished from the fragments via a constant 30 MeV kinetic energy cut and E^*, constructed via energy balance considerations, was *corrected* for collective expansion effects [9]. The data for each system was binned in terms of E^* in units of half an AMeV.

The basis of the present analysis lies in an examination of the fragment yield distribution in the context of Fisher's droplet formalism [10]. Fisher gives the number of droplets of size A normalized to the size of the system as:

$$n_A(\varepsilon) = q_0 A^{-\tau} \exp\left(\frac{A\Delta\mu}{T} - \frac{c_0 \varepsilon A^{\sigma}}{T}\right), \tag{1}$$

where τ is the topological critical exponent, for three dimensions $2 \leq \tau \leq 3$; q_0 is a normalization constant depending solely on τ [11]; $\Delta\mu = \mu - \mu_{coex}$ with μ as the chemical potential of the system and μ_{coex} as the chemical potential at coexistence; T is the temperature; σ is a critical exponent related to the ratio of the dimensionality of the surface to the volume; c_0 is the zero temperature surface energy coefficient; $\varepsilon = (T_c - T)/T_c$ is a measure of the distance from the critical point; and T_c is the critical temperature. This form of the surface energy is applicable only for $T \leq T_c$.

The fragment yields were fit to Eq. (1) modified to account for the Coulomb energy when a fragment moves from the liquid to the vapor (à la fission):

$$n_A = q_0 A^{-\tau} \exp\left(\frac{A\Delta\mu + E_{Coul}}{T} - \frac{c_0 \varepsilon A^{\sigma}}{T}\right), \tag{2}$$

where E_{Coul} is given by:

$$E_{Coul} = \frac{(Z_0 - Z)\,Z}{r_0\left((A_0 - A)^{1/3} + A^{1/3}\right)}\left(1 - e^{-x\varepsilon}\right). \tag{3}$$

Here $r_0 = 1.2$ fm. The term $1 - e^{-x\varepsilon}$ gives an account of the Coulomb energy behavior that vanishes as $x\varepsilon$ near T_c where no distinction exists between liquid and vapor. The fragment mass prior to decay was $A = 2Z(1 + y(E^*/B_f))$, where B_f is the binding energy of the fragment and y is a fit parameter that allows more or less decay. The temperature was determine via a degenerate Fermi gas, $T = \sqrt{E^*/\alpha}$, where $\alpha = 8(1 + (E^*/B_0))$ [12] to accommodate the empirically observed change in α with E^* [13]; B_0 is the binding energy of the fragmenting system. The total number of fragments N_A of size A was normalized to the size of the fragmenting system A_0, $n_A = N_A/A_0$.

For the ISiS data set, over 500 data points for $1.5 \leq E^* \leq 6.0$ AMeV and $5 \leq Z \leq 15$ were simultaneously fit to Eq. (2) with the parameters $\Delta\mu$, x, τ, σ, c_0 and T_c allowed to vary to minimize chi-squared. The secondary decay parameter was fixed at $y = 1$. Fragments with $Z < 5$ were not considered in the fit because Fisher's model expresses the

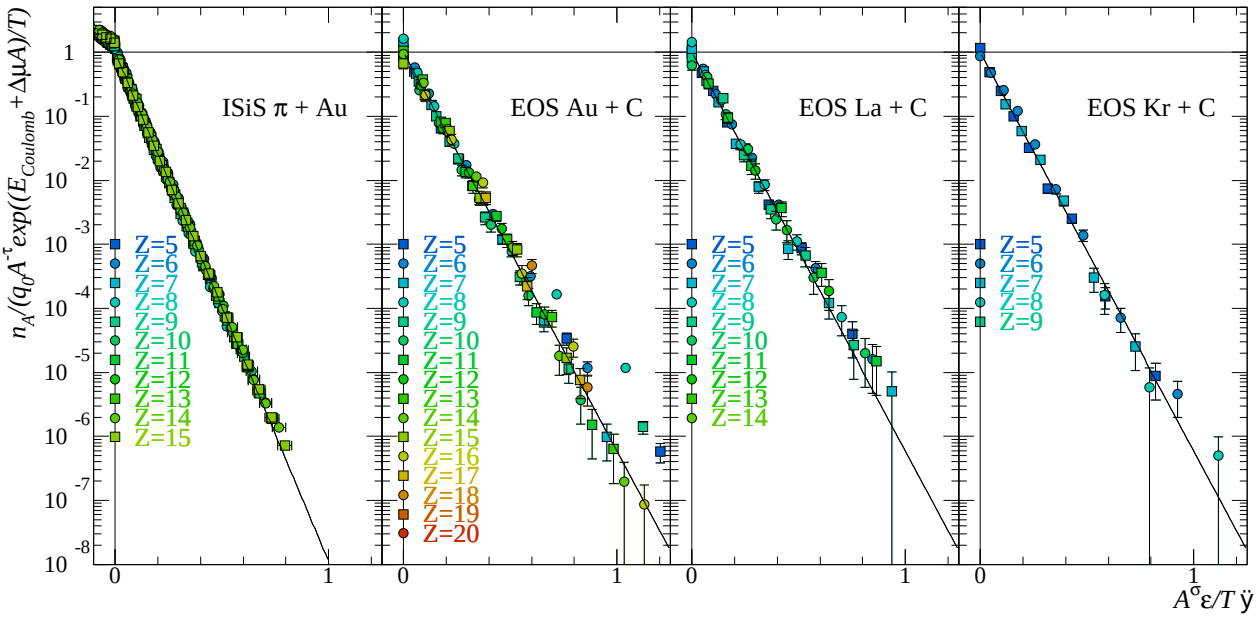

FIGURE 1. Left to right: The scaled fragment distributions of the ISiS gold data, the EOS gold, lanthanum and krypton data.

TABLE 2. Thermodynamic properties of excited nuclei

System	E_c^* (AMeV)	T_c (MeV)	ρ_c (ρ_0)	p_c (MeV/fm^3)	ΔH (MeV)	ΔE (AMeV)	C_c^F
ISiS π+ Au	3.8 ± 0.3	6.7 ± 0.2	~ 0.3	~ 0.07	26 ± 1	~ 15	0.25 ± 0.06
EOS Au + C	4.75 ± 0.25	7.7 ± 0.2	~ 0.36	~ 0.11	20.0 ± 0.9	~ 11	0.3 ± 0.1
EOS La + C	4.75 ± 0.25	7.7 ± 0.2	~ 0.36	~ 0.11	20.0 ± 0.9	~ 11	0.3 ± 0.1
EOS Kr + C	5.25 ± 0.25	8.2 ± 0.2	~ 0.37	~ 0.13	21.0 ± 1.0	~ 11	0.3 ± 0.1

mass/energy of a fragment in terms of bulk and surface energies and this approximation is known to fail for the lightest of nuclei where shell effects dominate. Aslo, for the lightest fragments equilibrium and non-equilibrium production cannot always be differentiated. Table 1 gives the resulting fit values. The value of τ and σ are close to the values expected for some three dimensional systems: $\tau \sim 2.2$ and $\sim 2/3$ and are in agreement with other multifragmentation results [14, 15]. The small positive $\Delta\mu$ value may indicate that the system is a super-saturated vapor. The value of c_0 is close to the value of the surface energy coefficient of the liquid-drop model: 16.8 MeV. The value of T_c is close to theoretical estimates [16]. Figure 1 shows the results of this analysis: the fragment mass yields are scaled by the power law pre-factor, the bulk term and the Coulomb energy: $n_A/q_0A^{-\tau}\exp(\Delta\mu A + E_{Coul}/T)$, and plotted against the temperature scaled by the surface energy: $A^{\sigma}\varepsilon/T$. The scaled data collapse to a single line over six orders of magnitude, precisely the behavior of a system undergoing a liquid-vapor transition. This line is the liquid-vapor coexistence line and provides direct evidence of the liquid-vapor transition in excited nuclei.

For the EOS data sets, E_c^*, listed in Table 2, was determined by the peak of the RMS fluctuations of the charge of the largest fragment normalized to Z_0, shown in Fig. 2. The values of E_c^* are close to previous observations in the EOS data [4, 9] and lead to T_c values that are comparable to theoretical estimates [16]. The topological exponent was fixed at $\tau = 2.2$ in keeping with the value for a variety of three dimensional systems [17] and myriad multifragmentation studies [1, 4]. There were 174 data points for 0.25 AMeV $\leq E^* \leq E_c^*$ and $5 \leq Z \leq Z_0/4$ from the three data sets simultaneously fit to Eq. (2). The parameters σ and c_0 were kept consistent between data sets while $\Delta\mu$, x and y were allowed to vary between them. The results are recorded in Table 1. The exponent values are in the range expected in Fisher's formalism for some three dimensional systems and are in agreement with those previously determined for the EOS [4] and ISiS gold multifragmentation data [15, 18], as expected for critical phenomena [19]. The surface energy coefficient c_0 is close to the value of the surface energy coefficient of the liquid-drop model. The differences in E_c^* and T_c between the ISiS and EOS data are due to the differences in differentiation between knockout particles and fragments; this difference leads to ${}^{EOS}E^* \approx 1.2\,{}^{ISiS}E^*$ [8] which accounts for the differing results; this difference affects all energy related quantities, e.g. c_0. The larger magnitude of $\Delta\mu$ values in the EOS results compared with the

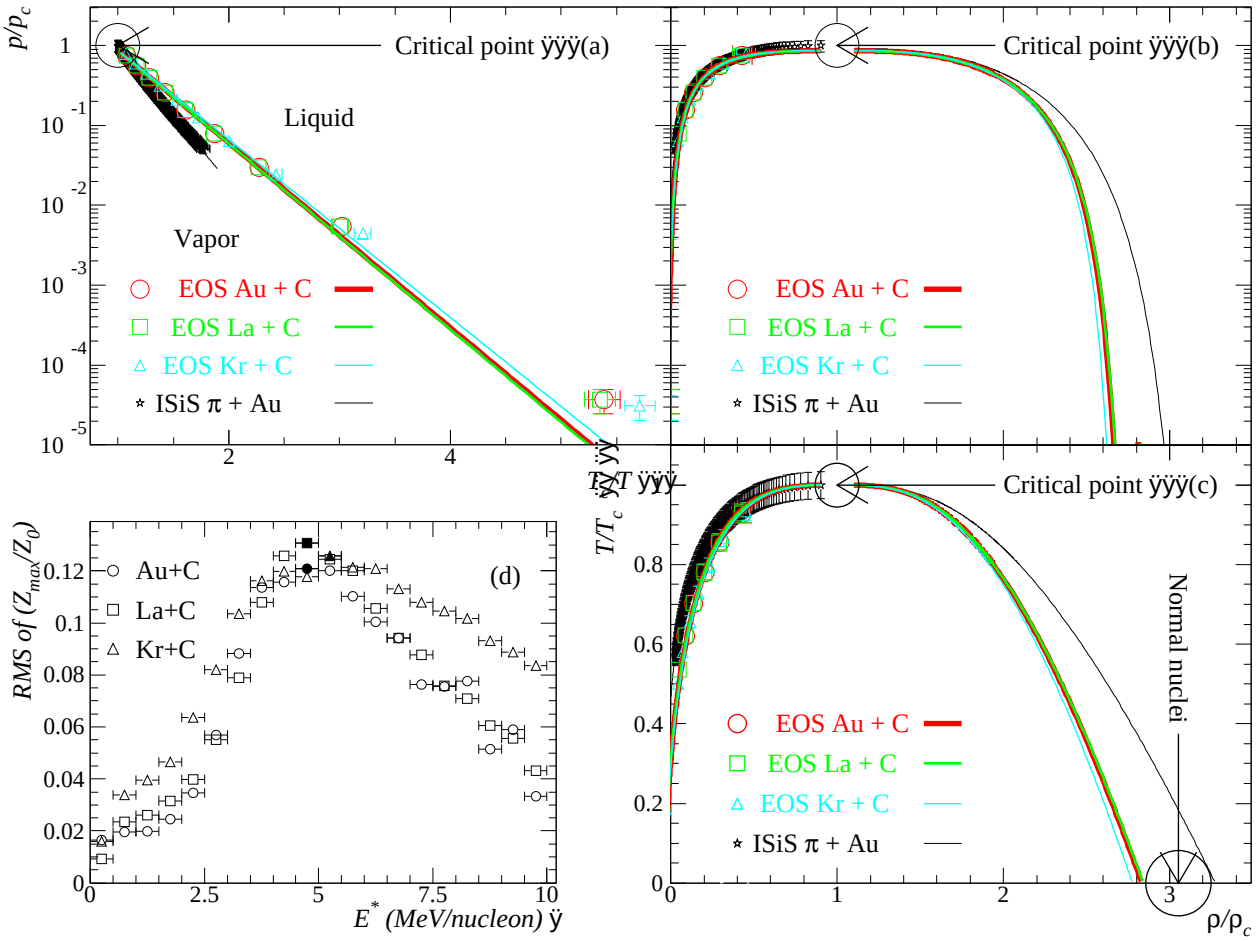

FIGURE 2. (a) The reduced pressure versus inverse reduced temperature, (b) the reduced pressure versus the reduced density and (c) the reduced temperature versus reduced density for the ISiS and EOS systems. (d) The RMS fluctuations of the charge of the largest fragment normalized to the charge of the fragmenting system versus excitation energy for the EOS systems, solid points show E_c^*.

ISiS results may be due to the greater degree of compression in the EOS collisions (nucleon on nucleon) compared to the ISiS collisions (π on nucleon). The Coulomb factor x is of the same order of magnitude for both experiments. The values of x may indicate more (Au and La) or less (Kr) Coulomb energy. The differences in the amount of secondary decay between the EOS and ISiS results is an open question. The EOS data scaled according to Eq. (2) shows data for all three systems collapsing onto a single line, Fig 1, illustrating the common nature of the underlying phenomenon.

Fisher assumed that a real gas of interacting particles could be treated as an ideal gas of non-interacting droplets; all of the non-ideality is accounted for in the clusterization. Thus the total pressure is found by summing the partial pressures $p/T = \sum n_A$ and the density is simply $\rho = \sum n_A A$. Accordingly, the reduced pressure is:

$$\frac{p}{p_c} = \frac{T \sum n_A(T)}{T_c \sum n_A(T_c)}. \tag{4}$$

The coexistence line for finite nuclear matter is obtained by using $n_A(T, \Delta\mu = 0, E_{Coul} = 0)$ from Eq. (2) in Eq. (4), transforming Fig. 1 into the familiar form shown in Fig. 2. The EOS gold and lanthanum data show nearly identical results due to their common T_c while the krypton data differs due to it's different T_c. The different slope for the ISiS and EOS data sets is due in part to the differing energy scales. An estimate of the bulk binding energy of nuclear matter was made by recalling the Clausius-Clapeyron equation $dp/dT = \Delta H/T\Delta V$ that leads to $p/p_c = \exp((\Delta H/T_c)(1-(T_c/T)))$ which describes several fluids up to T_c [20]. The slopes of the coexistence lines and values of T_c then give the molar enthalpy of evaporation of the liquid ΔH, shown in Table 2. The energy required to evaporate

a fragment, the bulk binding energy, is found from $\Delta H = \Delta E + pV = \Delta E + T$, since $pV = T$ for an ideal gas. Taking into account the average fragment size along the coexistence line, ~ 1.5 for ISiS, ~ 1.3 for EOS, gives the $\Delta E/$nucleon shown in Table 2. The value is close to the nuclear bulk energy coefficient of 15.5 AMeV. The values of ΔH and $\Delta E/$nucleon from the ISiS data differ form those of the EOS data, due in part to the differing measures of the E^* scale.

The reduced density of the vapor branch of the coexistence curve of finite nuclear matter is given by:

$$\frac{\rho}{\rho_c} = \frac{\sum A n_A(T)}{\sum A n_A(T_c)}. \tag{5}$$

This is shown in Fig. 2. It is possible to determine the high density branch as well: empirically, the ρ/ρ_c-T/T_c coexistence curves of several fluids can be fit with: [21]

$$\frac{\rho_{l,v}}{\rho_c} = 1 + b_1(1 - \frac{T}{T_c}) \pm b_2(1 - \frac{T}{T_c})^{\beta} \tag{6}$$

where the parameter b_2 is positive (negative) for the liquid ρ_l (vapor ρ_v) branch. The critical exponent β can be determined via: $\beta = (\tau - 2)/\sigma$ [10]. Table 1 shows the results. Fitting the coexistence curves of the ISiS and EOS data sets with Eq. (6) gives estimates of the full ρ_v branch of the coexistence curve. Changing the sign of b_2 gives the full ρ_l branch of the coexistence curve of finite nuclear matter. Assuming that normal nuclei exist at the $T = 0$ point of the coexistence curve in Fig. 2, then gives $\rho_c \sim \rho_0/3$.

Dividing Eq. (4) by Eq. (5) gives the critical compressibility factor $C_c^F = p_c/T_c\rho_c$. Table 1 shows the results for the ISiS and EOS data which are in agreement with values of several fluids [22]. The pressure at the critical point p_c can be found by using T_c and ρ_c in combination with C_c^F, the results are given in Table 2. This gives the a complete experimental measure of the critical point of finite nuclear matter (p_c, T_c, ρ_c) that agrees with theoretical calculations [16]. For completeness the p/p_c-ρ/ρ_c projection of the coexistence curve is determined and shown in Fig. 2.

Through a direct examination of accessible features of nuclear multifragmentation recorded by two different experiments for four different reactions a measurement of the coexistence curve of finite charged nuclear matter and estimates of the critical point have been made. The results for all systems agree, indicating that the phase diagram of nuclear matter based on experimental data has been established.

This work was supported by the US Department of Energy, the National Science Foundation, the National Science and Engineering Research Council of Canada, the Polish State Committee for Scientific Research, Indiana University Office of Research, the University Graduate School, Simon Fraser University and the Robert A. Welch Foundation.

REFERENCES

1. J. E. Finn *et al.*, Phys. Rev. Lett. **49**, 1321 (1982).
2. P. J. Siemens, Nature **305**, 410 (1983).
3. L. G. Moretto *et al.*, Phys. Rep. **287**, 249 (1997).
4. J. B. Elliott *et al.*, Phys. Rev. C **62**, 064603 (2000).
5. J. Pochodzalla *et al.*, Phys. Rev. Lett **75**, 1040 (1995).
6. M. D'Agostino *et al.*, Phys. Lett. B **473**, 219 (2000).
7. K. Kwiatkowski *et al.*, NIM **A**360, 571 (1995).
8. T. Lefort *et al.*, Phys. Rev. Lett **83**, 4033 (1999).
9. J. A. Hauger *et al.*, Phys. Rev. C **62**, 024626 (2000).
10. M. E. Fisher, Physics **3**, 255 (1967).
11. H. Nakanishi and H. E. Stanley, Phys. Rev. B **22**, 2466 (1980).
12. A.H. Raduta *et al.*, Phys. Rev. C **55**, 1344 (1997).
13. K. Hagel *et al.*, Nucl. Phys. **A486**, 429 (1988).
14. M. D'Agostino *et al.*, Nucl. Phys. A **650**, 328
15. M. Kleine Berkenbusch *et al.*, nucl-th/0109062 (2001).
16. J. N. De *et al.*, Phys. Rev. C **59**, R1 (1999).
17. D. Stauffer and A. Aharony, "Introduction to Percolation Theory", 2nd ed. (Taylor and Francis, London, 2001).
18. J. B. Elliott *et al.*, to be published in Phys. Rev. Lett. (2001).
19. J. M. Yeomans, "Statistical Mechanics of Phase Transitions", 1rst ed. (Clarendon Press, Oxford 1992).
20. E.A. Guggenheim, "Thermodynamics", 4th ed. (North-Holland, 1993).
21. E. A. Guggenheim, J. Chem. Phys., **13**, 253 (1945).
22. C. S. Kiang, Phys. Rev. Lett. **24**, 47 (1970).